STEM CELLS®

TISSUE-SPECIFIC STEM CELLS

Cell Mechanosensitivity to Extremely Low-Magnitude Signals Is Enabled by a LINCed Nucleus

GUNES UZER,[a] WILLIAM R. THOMPSON,[b] BUER SEN,[a] ZHIHUI XIE,[a] SHERWIN S. YEN,[a] SEAN MILLER,[a] GUNIZ BAS,[a] MAYA STYNER,[a] CLINTON T. RUBIN,[c] STEFAN JUDEX,[c] KEITH BURRIDGE,[d] JANET RUBIN[a]

Key Words. Mesenchymal stem cells • Vibration • Strain • Nucleus • Nesprin • FAK • Akt • RhoA

[a]Department of Medicine, University of North Carolina, Chapel Hill, North Carolina, USA; [b]School of Physical Therapy, Indiana University, Indianapolis, Indiana, USA; [c]Department of Biomedical Engineering, State University of New York, Stony Brook, New York, USA; [d]Department of Cell Biology and Physiology, University of North Carolina, Chapel Hill, North Carolina, USA

Correspondence: Gunes uzer, Ph.D., 5030 Burnett-Womack Building, Chapel Hill, North Carolina 27599, USA. Telephone: 919–966-6743; Fax: 919- 806-2181; e-mail: gunes_uzer@med.unc.edu

Received September 29, 2014; accepted for publication February 19, 2015; first published online in STEM CELLS *EXPRESS* March 18, 2015.

1066-5099/2014/$30.00/0

http://dx.doi.org/10.1002/stem.2004

ABSTRACT

A cell's ability to recognize and adapt to the physical environment is central to its survival and function, but how mechanical cues are perceived and transduced into intracellular signals remains unclear. In mesenchymal stem cells (MSCs), high-magnitude substrate strain (HMS, ≥2%) effectively suppresses adipogenesis via induction of focal adhesion (FA) kinase (FAK)/mTORC2/Akt signaling generated at FAs. Physiologic systems also rely on a persistent barrage of low-level signals to regulate behavior. Exposing MSC to extremely low-magnitude mechanical signals (LMS) suppresses adipocyte formation despite the virtual absence of substrate strain (<0.001%), suggesting that LMS-induced dynamic accelerations can generate force within the cell. Here, we show that MSC response to LMS is enabled through mechanical coupling between the cytoskeleton and the nucleus, in turn activating FAK and Akt signaling followed by FAK-dependent induction of RhoA. While LMS and HMS synergistically regulated FAK activity at the FAs, LMS-induced actin remodeling was concentrated at the perinuclear domain. Preventing nuclear-actin cytoskeleton mechanocoupling by disrupting linker of nucleoskeleton and cytoskeleton (LINC) complexes inhibited these LMS-induced signals as well as prevented LMS repression of adipogenic differentiation, highlighting that LINC connections are critical for sensing LMS. In contrast, FAK activation by HMS was unaffected by LINC decoupling, consistent with signal initiation at the FA mechanosome. These results indicate that the MSC responds to its dynamic physical environment not only with "outside-in" signaling initiated by substrate strain, but vibratory signals enacted through the LINC complex enable matrix independent "inside–inside" signaling. STEM CELLS *2013;33:2063–2076*

INTRODUCTION

Since the beginning of life, mechanical cues have guided cell fate and function. The role of mechanical signaling in defining cell fate is evidenced in the pluripotent mesenchymal stem cells (MSC) that regenerate and repair tissues [1, 2]. Lineage guidance of MSCs relies in-part on physical cues derived from the environment [3]. Strain of bone and muscle during daily activity suppresses adipogenesis [4], while promoting osteogenesis [5] and myogenesis [6]. In vitro, when cells are attached to an extracellular matrix, mechanical cues derived from substrate deformation or quality (e.g., stiffness and topology) can be transmitted through focal adhesion (FA) connections to initiate signal pathways that cause reorganization of cytoskeletal structure [7, 8] and allow automodulation of signal strength transmission to the nucleus [9]. Mimicking exercise, in vitro application of high-magnitude substrate strain (HMS, ≥2%) effectively suppresses adipogenesis via induction of focal adhesion kinase (FAK)/mTORC2/Akt signaling generated at FAs [10]. Physical signals that regulate biologic functions, however, do not necessarily need to be large to be influential. Physiologic systems ranging from hair cells responding to sound in the cochlea [11] to circadian rhythms of Drosophila [12] rely on a persistent barrage of low magnitude, high-frequency signals. Moreover, application of high frequency, low-magnitude mechanical signals (LMS) copy high-impact exercises to improve musculoskeletal function [13, 14], decrease adipose encroachment in the bone marrow in vivo [1, 15] and augment MSC osteogenesis [16] while decreasing adipogenesis [17] in vitro. In contrast to HMS signaling that depends on matrix strain, the mechanism by which LMS is perceived and induces relevant signaling pathways in cells is not clear.

Despite their physiologic relevance, little is known about how very small signals, such as LMS, are perceived at the cell or nuclear level to control function [18]. LMS creates a complex local loading environment that depends on many factors including frequency, amplitude, and viscosity [19]. Peak strains generated

by LMS are on the order of approximately 1–2 micro strain ($\mu\varepsilon$) [20] while cell responses linked to HMS are usually applied at $\geq$10,000 $\mu\varepsilon$ [7, 21, 22], suggesting that substrate deformation does not contribute to the LMS response. Current literature addressing how cells sense vibration is focused on computational analyses or correlations that do not directly speak to the mechanisms responsible for the cell response to vibration [23–26]; indeed research has been largely limited to functional outcome assays describing cell osteogenesis, adipogenesis, proliferation, or tissue/organism level response [27–55].

Remodeling its cytoskeleton in response to the surrounding physical environment allows the cell to actively participate in the mechanoregulation of cell fate and function [56]. Not only does internal cell tension driven by RhoA activity directly modulate cell differentiation [57] but mechanically guided cytoskeletal remodeling alters signal transmission [58]. For example, HMS induced remodeling of the MSC actin cytoskeleton, enhances connections through new FA complexes, and results in amplification of mechanically generated signals in response to repeated force [10], thus more efficiently suppressing MSC adipogenesis. Scaling the same analogy to the organismal level, shorter but repeated exercise durations have shown to be more effective in improving glycemic control compared with a single longer duration [59]. Not surprisingly, repeated exposure to LMS was also more effective than a single bout in controlling MSC lineage decisions [17], presumably due to adaptive remodeling of cell structure[16, 55].

Ultimately, mechanical force influences the nuclear transcriptional machinery via physical and biochemical means [60–62]. The mechanical connection between the cytoskeleton and the nucleus is transferred via the linker of nucleoskeleton and cytoskeleton (LINC) complex [63, 64]. LINC-associated giant isoforms of Nesprin-1 and Nesprin-2 bind actin filaments through their N-termini [65, 66] and SUN proteins via their C-terminal KASH (Klarsicht, ANC-1, Syne Homology) domains [67]. LINC complexes form a filamentous network on the nuclear surface [68], perhaps akin to focal adhesions [69, 70], where force can dynamically alter LINC mediated mechanocoupling between nucleus and cytoskeleton [71, 72]. LINC mediated force has been shown to regulate nuclear structure and function [73, 74]. Pathologic alterations in the nuclear structure, including lamin mutations common to progeria and depletion or dislocation of giant Nesprins, disrupt LINC connections [64, 75] to interfere with cellular processes including proliferation [76], migration [64], and differentiation [77]. Recently, forces applied via Nesprin bound magnetic beads were shown to cause phosphorylation of the Lamin/LINC binding partner Emerin resulting in increased nuclear stiffness [78].

The cytoplasmic cytoskeleton, connected to substrate via peripheral focal adhesions, spans through F-actin stress fibers to attach to LINC on the outer nuclear membrane, in this way transmitting forces from outside the cell inwards [79]. In smooth muscle cells, dissection of a single apical actin stress fiber generates a force of 65 nN on the nucleus [80]. Switching between weak and strong LINC-actin coupling states can generate up to 40 nN force differentials which are an order of magnitude larger than the cytoskeletal forces required to initiate F-actin assembly and signaling (approximately 10–50 pN) [81]. This suggests that forces generated by LINC-actin coupling alone should be able to generate sufficient internal force from inside the cell to initiate signaling events. The positive correlation between rate of acceleration and LMS response [23] suggests the possibility that the nucleus might participate in LMS-induced signaling as a passive structural element by virtue of its denser/stiffer nature. We previously explored this possibility in silico and found that LMS-induced accelerations caused relative nuclear motions that were 100–1,000 times larger than those generated by LMS-induced fluid shear stresses [26]. Supportive of the hypothesis that nucleus might participate in the sensing of vibratory signals, Sun1$^{-/-}$ mice gradually become deaf [82], thus strengthening the notion that LINC may be important for vibrational sensing, including sound.

Here, using biochemical and imaging techniques, we approach the question of how LMS generates signaling, considering whether LMS and HMS use same signaling mechanisms to initiate cell response. We address whether LMS or HMS are perceived in the same way and, more specifically, ask if LMS directed signaling and regulation of MSC differentiation require LINC facilitated mechanical coupling between the nucleus and cytoskeleton.

Experimental Design

MSCs were seeded at 100,000 per well in six-well polystyrene plates (LMS) or in Bioflex Collagen-I coated silicone plates [17] (HMS, LMS, or LMS+HMS). LMS was applied one time (1×), and repeated after a 2-hour rest period (2×) in the form of high-frequency low-magnitude vibration of 0.7 g (1 g = Earth's gravitational field) at 90 Hz for 20 minutes at room temperature (RT). HMS was applied as a uniform uniaxial strain of 2% at 0.17 Hz for 20 minutes at RT. First, we studied the LMS-induced FAK phosphorylation (p-FAK, Tyr397) events by a time course study to test whether 1× LMS served to augment the second (2×) LMS. We then investigated the cellular adaptations following 1× LMS by FA isolation and RhoA activation assays. We further tested whether p-FAK was necessary for the RhoA activity via PF573228 (3 μM) pretreatment. We then asked whether activating RhoA alone via lysophosphatidic acid (LPA, 30 μM) also amplifies subsequent LMS response. Alternatively, we also tested whether HMS and LMS work synergistically to amplify each other using combinations of LMS+HMS. Role of the cytoskeleton in facilitating LMS-induced FAK activation was tested by disrupting the actin and microtubule cytoskeletons as well as cellular tension via pretreatment of Cytochalasin-D (0.2 μM), Colchicine (1 μM), and Y27632 (10 μM). We used immunofluorescence to determine whether LMS causes rearrangement of the actin cytoskeleton.

To test whether LINC-mediated mechanocoupling of nucleus and cytoskeleton was required for LMS mechanoresponse, we measured LMS induced FAK and Akt activation as well as modulation of MSC adipogenesis after the nuclear envelope LINC complex was disrupted by siRNA treatment of SUN1 and 2 [63] or by overexpression of a dominant negative form of Nesprin KASH domain [64]. A role of Emerin in LMS signaling was queried using a targeting siRNA. Finally, to identify differences in proximal signaling due to LMS and HMS, mechanically activated Akt was quantified by blocking FAK activity or use of siRNA targeting the FAK comodulator Fyn [21].

Materials and Methods

MSC Isolation

Marrow derived mesenchymal stem cells (MSCs) from 8 to 10 week male C57BL/6 mice were prepared after Peister et al. [83]. Tibial and femoral marrow were collected in RPMI-1640, 9% fetal bovine serum (FBS), 9% HS, 100 μg/ml penicillin/streptomycin, and 12 μM L-glutamine. After 24 hours, nonadherent cells were removed by washing with phosphate-buffered saline (PBS) and adherent cells cultured for 4 weeks. Passage 1 cells were collected after incubation with 0.25% trypsin/1 mM EDTA $\times$ 2 minutes, and replated in a single 175-cm^2 flask. After 1–2 weeks, passage 2 cells were replated at 50 cells per square centimeter in expansion medium (Iscove modified Dulbecco's, 9% FBS, 9% HS, antibiotics, L-glutamine). MSC were re-plated every 1–2 weeks for two consecutive passages up to passage 5 and tested for osteogenic and adipogenic potential, and subsequently frozen.

Application of LMS and Strain

Vibrations were applied to MSCs at peak magnitudes of 0.7 g at 90 Hz for 20 minutes at RT [17]. Controls were sham handled. Unless stated otherwise, LMS was applied as two 20 minutes bouts separated by 2 hours rest. Uniform 2% biaxial strain was delivered at 10 cycles per minute for 20 minutes to MSCs using the Flexcell FX-4000 system (Flexcell International, Hillsborough, NC, www.flexcellint.com).

Cell Culture and Pharmacological Reagents

FBS was obtained from Atlanta Biologicals (Atlanta, GA, http://www.atlantabio.com/). Culture media, trypsin-EDTA, antibiotics, and Phalloidin-Alexa-488 were from Invitrogen (Carlsbad, CA, www.invitrogen.com). KU63794, PF573228, Y27632, Colchicine, and Cytochalasin D were purchased from Sigma Aldrich (St. Louis, MO, www.sigmaaldrich.com). LPA was purchased from Cayman Chemicals (Ann Arbor, MI, www.caymanchem.com). MSCs [84] were maintained in IMDM with FBS (10%, v/v) and penicillin/streptomycin (100 μg/ml). For phosphorylation and RhoA activity, seeding density was 10,000 cells per square centimeter and 2,500 cells per square centimeter for immunostaining experiments. All the groups were cultured for 48 hours before beginning experiments and were serum starved overnight in serum free medium. LPA (30 μM) was added 2 hours before LMS. All other pharmacological inhibitors were added 1 hour before either LMS or Strain at the following concentrations: Cytochalasin D (0.2 μM), Y27632 (10 μM), Colchicine (1 μM), PF573228 (3 μM), and KU63794 (2 μM).

For adipogenic differentiation experiments, marrow-derived MSCs were plated at a density of 100,000 cell per well into six-well culture plates and treated with either with siRNA against *SUN-1* and *SUN-2* (siSUN) or with pCDH-EF1-MCS1-puro-mCherry-Nesprin-1αKASH (DNKASH) plasmids using 1 μg DNA per 100,000 cell (proper controls were used for both treatments). Eighteen hours after the transfection, growth medium was replaced with adipogenic medium containing 0.1 μM dexamethasone and 5 μg/ml insulin. Cultures were incubated for 5 days with or without LMS treatment (2 $\times$ 20 minutes per day separated by 2 hours).

Overexpression and Knockdown Sequences

pCDH-EF1-MCS1-puro-mCherry (mCherry control) and DNKASH plasmids were kindly provided by Dr. Lammerding [85]. MSCs were transfected using 1 μg DNA per 100,000 cells using LipoD293 transfection reagent (SignaGen Laboratories, Rockville, MD, www.signagen.com) according to manufacturer's instructions. Seventy-two hours after the initial transfection, stably transfected cells were selected using 10 μg/ml puromycin. For transiently silencing specific genes, cells were transfected with gene-specific small interfering RNA (siRNA) or control siRNA (20 nM) using PepMute Plus transfection reagent (SignaGen Labs) according to manufacturer's instructions. Strain or LMS were applied 72 hours after initial transfection. The following Stealth Select siRNAs (Invitrogen) were used in this study: negative control for *SUN-1* 5′- GAAATCGAAGTACCTCGAGTGATAT −3′; *SUN-1* 5′- GAAAGGCTATGAATCCAGAGCTTAT-3′; negative control for *SUN-2* 5′-CACCAGAGGCTAGAACTCTTACTCA-3′; *SUN-2* 5′-CACCAAGACTCGGAAGATCTCTTCA-3′; negative control for *Fyn* 5′-GCCUCGUACAGAAGAAACGCCGAAU-3′; *Fyn* 5′-UAAAGCGCC ACAAACAGUGUCACUC-3′; negative control for *Emerin* 5′-CAACCCUUACUCG-GGUAUCUAGGUG-3′; *Emerin* 5′-CAACAUCCCU-CAUGGGCCUAUUGUG-3′.

Isolation of Focal Adhesions

Cells were incubated with triethanolamine (TEA)-containing low ionic-strength buffer (2.5 mM TEA, pH 7.0) for 3 minutes at RT, 1$\times$ PBS containing protease/phosphatase inhibitors. A Waterpik (Fort Collins, CO, www.waterpik.com) nozzle held 0.5 cm from the plate surface at approximately 90° supplied the hydrodynamic force to flush away cell bodies, membrane-bound organelles, nuclei, cytoskeleton, and soluble cytoplasmic materials [86] so that residual focal adhesions could be isolated.

Isolation of Nuclear Envelope Proteins

MSCs were plated on one-well (100 cm^2, Greiner Bio-One, NC, www.gbo.com) at 10,000 cell per square centimeter. Nuclear envelope proteins were extracted using Minute Nuclear Envelope Protein Extraction Kit (Invent biotech, Germany, www.inventbiotech.com) according to manufacturer's instructions using at least ten million cells per group.

Real-Time PCR

Total RNA was isolated using the RNeasy mini kit (QIAGEN, Valencia, CA, www.qiagen.com) and treated with deoxyribonuclease I to remove contaminating genomic DNA. Reverse transcription was performed with 1 μg RNA in a total volume of 20 μl per reaction. Real-time polymerase chain reaction (PCR) was performed on a Bio-Rad iCycler (Bio-Rad Laboratories, Inc., Hercules, CA, www.bio-rad.com). Twenty-five-microliter amplification reactions contained primers at 0.5 μm, deoxynucleotide triphosphates (0.2 mm each) in PCR buffer, and 0.03 U Taq polymerase along with SYBR-green (Molecular Probes, Inc., Eugene, OR, http://www.lifetechnologies.com) at 1:150,000. Aliquots of cDNA were diluted 5- to 5000-fold to generate relative standard curves with which sample cDNA was compared. Standards and samples were run in triplicate. PCR products from all species were normalized for the amount of *18S* amplicons. Primer sequences as follows adiponectin (*APN*, Forward:5′-GCAGAGATGGCA CTCCTGGA-3′, Reverse:5′-CCCTTCAGCTCCTGTCATTCC-3′), Fatty acid binding protein 4 (*AP-2*, Forward:5′-CATCAGCG-TAAATGGGGATT-3′, Reverse:5′-TCGACTTTCCATCCCACTTC-3′), Peroxisome proliferator-activated receptor gamma (*PPAR*γ, Forward:5′-GCTTATTTAT-GATAGGTGTGATC-3′, Reverse:5′-GCATTGTGAGACATCCCCAC-3′) expressions were normalized to and *18S* (Forward:5′-GAACGTCTGCCCTATCAACT-3′, Reverse:5′-CCAAGATCCAACTACGAGCT-3′).

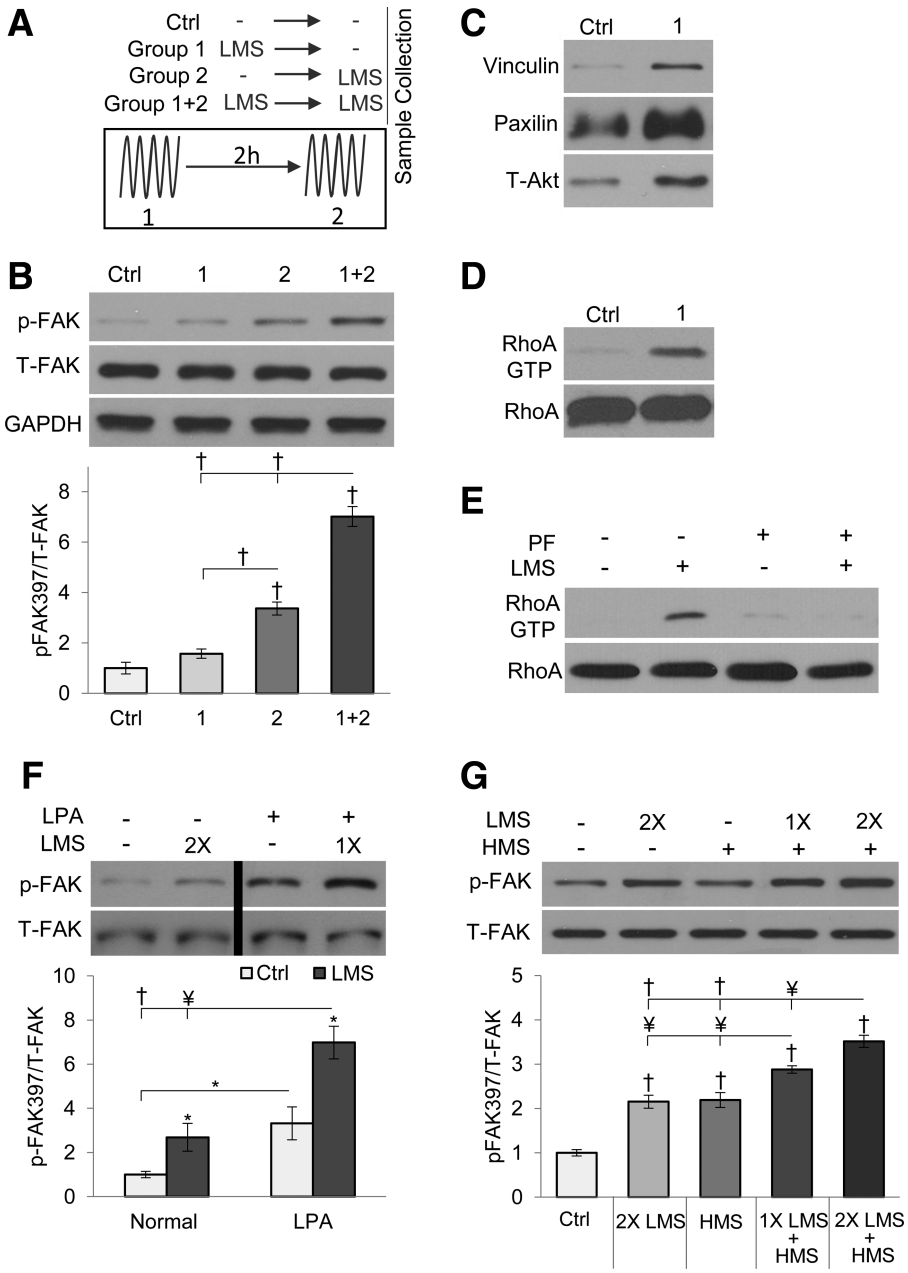

Figure 1. RhoA enhanced cytoskeleton modulates low-magnitude mechanical signal (LMS)-induced focal adhesion kinase phosphorylation (p-FAK). **(A):** Schematic representation of time course experiment depicting different groups. Groups (1) and (2) were subjected to single LMS with or without a 2-hour rest, respectively. Group (1 + 2) was subjected to both LMS treatments. **(B):** LMS acutely increased p-FAK to 3.4-fold ($p < 0.001$); 2 hours later p-FAK was not significantly different than control. Reapplication of LMS resulted in sevenfold increase, doubling the single LMS response. **(C):** Isolation of focal adhesion (FAs) 2 hours after a single LMS treatment was subject to Western blot analysis; increased total vinculin, paxillin, and Akt were consistent with increased FAs. **(D):** FA increase was accompanied by RhoA activity, and **(E)** RhoA activity was dependent on initial LMS-induced FAK activity as FAK inhibitor PF573228 (PF, 3 μM) prevented LMS-activated RhoA. **(F):** RhoA activated with lysophosphatidic acid (LPA) (30 μM) increased p-FAK threefold ($p < 0.05$); following LPA, a single LMS application increased p-FAK response by sevenfold ($p < 0.001$). The black bar on the representative Western blot indicates that it has been cropped to change the sample positions. **(G):** LMS amplified the high-magnitude substrate strain (HMS) response: 1 and 2× LMS pretreatment synergistically augmented the HMS response by 30% ($p < 0.01$) and 60% ($p < 0.01$), respectively. *, $p < 0.05$; ¥, $p < 0.01$; †, $p < 0.001$, against control and each other. Abbreviations: Ctrl, control; GADPH, Glyceraldehyde 3-phosphate dehydrogenase; HMS, high-magnitude substrate strain; LMS, low-magnitude mechanical signal; LPA, lysophosphatidic acid; PF, PF573228; p-FAK, focal adhesion kinase phosphorylation; T-FAK, total focal adhesion kinase protein.

Western Blotting

Whole cell lysates were prepared using an radio immunoprecipitation assay lysis buffer (150 mM NaCl, 50 mM Tris HCl, 1 mM EDTA, 0.24% sodium deoxycholate,1% Igepal, pH 7.5) to protect the samples from protein degradation NaF (25 mM), Na_3VO_4 (2 mM), aprotinin, leupeptin, pepstatin,

and phenylmethylsulfonylfluoride (PMSF) were added to the lysis buffer. Whole cell lysates (20 μg) were separated on 7%-12% polyacrylamide gels and transferred to polyvinylidene difluoride membranes. Membranes were blocked with milk (5%, w/v) diluted in Tris-buffered saline containing Tween20 (TBS-T, 0.05%). Blots were then incubated overnight at 4°C with appropriate primary antibodies. Following primary antibody incubation, blots were washed and incubated with horseradish peroxidase-conjugated secondary antibody diluted at 1:5,000 (Cell Signaling, Danvers, MA, www.cellsignal.com) at RT for 1 hour. Chemiluminescence was detected with ECL plus (Amersham Biosciences, Piscataway, NJ, www.gelifesciences.com). At least three separate experiments were used for densitometry analyses of western blots and densitometry was performed via NIH ImageJ software.

RhoA Activation Assay

Purification of recombinant proteins and construction of the pGEX4T-1 prokaryotic expression constructs containing the Rho-binding domain (RBD) of Rhotekin has been described [87]. Briefly, expression of the fusion proteins in *Escherichia coli* was induced using isopropyl β-D−1-thiogalactopyranoside (100 μM) for 12–16 hours at RT. Bacterial cells were lysed in lysis buffer containing Tris HCl (50 mM, pH 7.6), NaCl (150 mM), MgCl2 (5 mM), dithiothreitol (1 mM), aprotinin (10 μg/ml), leupeptin (10 μg/ml), and PMSF (1 mM). Recombinant proteins were purified by incubation with glutathione-sepharose 4B beads (GE Healthcare, Piscataway, NJ, http://www.gehealthcare.com/) at 4°C. Pull down of active RhoA, using glutathione-*S*-transferase-RBD (GST-RBD) beads, was performed as described [88]. MSC cells were lysed in buffer containing Tris HCl (50 mM, pH 7.6), NaCl (500 mM), Triton X-100 (1%, v/v), SDS (0.1%, v/v), sodium deoxycholate (0.5%, w/v), $MgCl_2$ (10 mM), orthovanadate (200 μM), and protease inhibitors. Lysates were clarified by centrifugation, equalized for total volume and protein concentration, and rotated at 4°C for 30 minutes with 50 μg of purified GST-RBD bound to glutathione-sepharose beads. The bead pellets were washed in lysis buffer three times, followed by pelleting of the beads by centrifugation between each wash, and subsequently processed by SDS-polyacrylamide gel electrophoresis.

Immunofluorescence

Following strain or LMS treatment, cells were fixed with paraformaldehyde. For Nesprin-2 staining, cells were incubated in anti-Nesprin-2 (kindly provided by Dr. Hodzic) [89] primary antibody solution (0.5%, v/v in blocking serum) for 24 hours at 4°C, followed by secondary antibody incubation DyLight 649 AffiniPure Donkey Anti-Mouse IgG (Jackson Immuno Research Laboratories, West Grove, PA, www.jacksonimmuno.com). For actin staining, cells were incubated with phalloidin-conjugated Alexa Fluor-488 (Invitrogen).

Statistical Analysis

Results were presented as mean ± SEM. Densitometry analyses were performed on at least three separate experiments. Differences between groups were identified by one-way analysis of variance (ANOVA) followed by Newman-Keuls post hoc tests. Interactions between two different treatments were evaluated using two-way ANOVA. $p < 0.05$ were considered significant.

Results

Repeated LMS Exposures Generate RhoA-Reinforced Cell Structure to Augment Mechanically Induced FAK Activity

We investigated LMS mechanotransduction, asking whether it differed from that induced by HMS where substrate strain triggers FAK activation [21] at FA mechanosomes [90, 91]. To test whether FAK situated at FAs was involved in LMS signaling, we performed a detailed time course experiment. As illustrated in Figure 1A, Group 1 is subjected to a single LMS (0.7 g, 90 Hz, 20 minutes) and p-FAK measured 2 hours after (before second LMS), Group 2 is subjected to LMS and p-FAK measured immediately. Group 1+2 received both LMS treatments with p-FAK measured after the second LMS. Experiments were timed such that all the samples were collected at the same time. p-FAK increased 3.4-fold ($p < 0.001$) immediately after LMS but, shown in Figure 1B, returned to baseline levels after 2 hours ($p < 0.001$) where it was not significantly elevated compared with control. A prior application of LMS, however, augmented a second LMS (1+2) by two-fold compared with single application alone ($p < 0.001$). This suggests generation of an amplification mechanism in response to the first LMS.

We previously showed that HMS triggered cytoskeletal adaptations amplify signaling responses to subsequent mechanical challenges [10]. To elucidate the amplification mechanism resulting from the first LMS signal, we asked whether, similar to HMS [7], LMS induced focal adhesions and RhoA activity. Immediately before the second LMS application (group 1, 2 hours after LMS) there were more focal adhesions as measured by Western blot analysis of substrate attached FAs [7, 86] against vinculin, paxilin, and t-Akt (Fig. 1C). We also observed increased RhoA activity 2 hours after the first application of LMS (Fig. 1D). These finding suggest that similar to HMS [10], LMS increases cytoskeletal remodeling and strengthens FA substrate connections. Importantly, p-FAK activity was *required* for LMS activation of RhoA; pharmacologic inhibition of FAK (PF573228, 3 μM) prevented LMS-induced RhoA activation (Fig. 1E).

To confirm that the LMS signal response could be enhanced by an increased cytoskeleton, we delivered LMS after treatment with LPA, which increases actin bundling through RhoA activation (Supporting Information Fig. S1). LPA increased basal p-FAK by threefold and a single LMS application further increased p-FAK by twofold ($p < 0.001$, Fig. 1F). Two-way ANOVA showed that both LPA and LMS significantly affect the outcome ($p < 0.001$) but no significant interaction was detected ($p = 0.102$).

As both HMS [7] and LMS (Fig. 1C) elicited increased focal adhesions and an LPA-induced cytoskeleton served to amplify LMS signaling (Fig. 1F), we asked whether LMS induced cytoskeletal change could synergistically amplify FAK signaling situated at the focal adhesions. Depicted in Figure 1G, MSCs were treated with one (1×) or two (2×) bouts of LMS followed by HMS. While a single HMS (2% uniaxial strain, 0.17 Hz, 20 minutes) and 2× LMS induced comparable elevation of p-FAK relative to control (2.1-fold each, $p < 0.001$), pretreatment with LMS augmented the HMS response. Pretreating MSC's with 2× LMS before HMS yielded the largest p-FAK response compared with control (3.5-fold, $p < 0.001$); this response was higher than both HMS alone (60% $p < 0.001$)

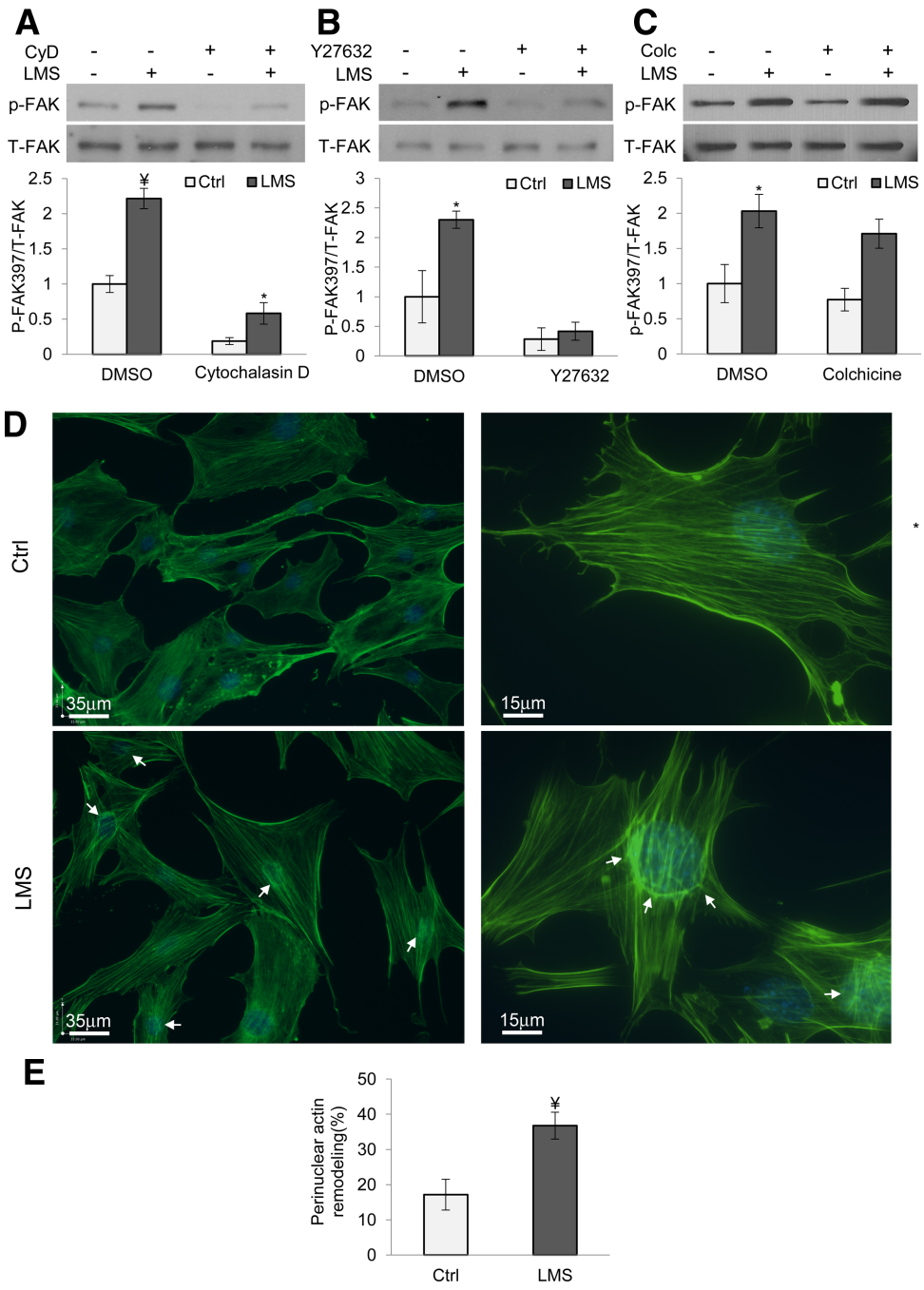

Figure 2. Low-magnitude mechanical signal (LMS) signaling requires an intact actin cytoskeleton and induces actin rearrangement at the perinuclear domain. Depolymerizing actin with **(A)** Cytochalasin D (CyD, 0.2 μM) decreased both basal and LMS-induced focal adhesion kinase phosphorylation (p-FAK) ($p < 0.001$). **(B):** Inhibiting RhoA activity with ROCK inhibitor Y27632 (10 μM) ablated p-FAK due to LMS ($p < 0.001$). **(C):** Inhibiting microtubule polymerization with colchicine (1 μM) did not change the LMS response. **(D):** LMS treatment induced actin rearrangement around cell nucleus 1 hour later (arrows). Nuclear straining (4′,6-diamidino-2-phenylindole, DAPI) was merged with actin images to clarify nuclear position. **(E):** Quantification of cells exhibiting actin staining around perinuclear domain revealed that LMS increased this frequency from 17% (Control, $n = 250$) to 36% ($p < 0.01$, $n = 500$). *, $p < 0.05$; ¥, $p < 0.01$; †, $p < 0.001$, against control and each other. Abbreviations: Colc, colchicines Ctrl, control; CyD, Cytochalasin D; DAPI, 4′,6-diamidino-2-phenylindole; DMSO, dimethyl sulphoxide; LMS, low-magnitude mechanical signal; p-FAK, focal adhesion kinase phosphorylation; T-FAK, total focal adhesion kinase protein.

and that following a single LMS pretreatment (32% $p < 0.01$). Synergistic regulation of p-FAK activity through LMS and HMS ($p < 0.001$, two-way ANOVA) supports that LMS treatment results in more robust cytoskeleton terminating in FAs, where HMS is known to initiate signaling in MSCs [21].

LMS Induced p-FAK Requires an Intact Actin Cytoskeleton that Reorganizes at the Perinuclear Domain

To further implicate the cytoskeleton in the response to LMS, we asked if an intact cytoskeleton was required for LMS activation of FAK. MSCs treated with the actin polymerization

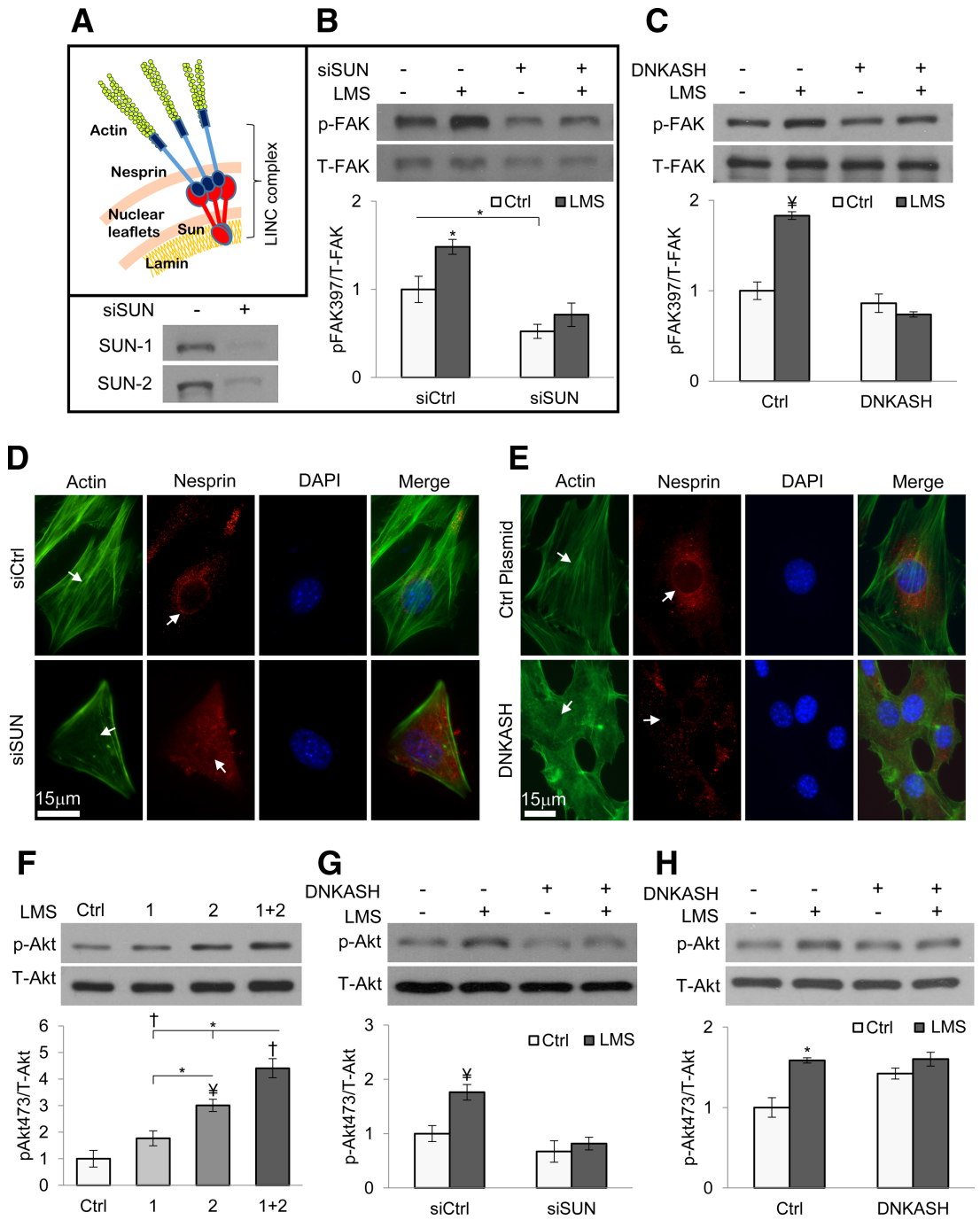

Figure 3. Linker of nucleoskeleton and cytoskeleton (LINC)-mediated actin-nuclear connectivity is required for low-magnitude mechanical signal (LMS) signaling. **(A):** Mechanically decoupling LINC from the cytoskeleton through inhibition of Nesprin localization to the nuclear envelope by either **(B)** siRNA repression of SUN expression (both SUN-1 and SUN-2) or **(C)** overexpressing a dominant negative KASH domain (pCDH-EF1-MCS1-puro-mCherry-Nesprin-1αKASH [DNKASH]) prevented LMS-induced FAK activation. **(D):** siRNA against SUN-1 and SUN-2 (siSUN) and **(E)** DNKASH treatments diminished Nesprin staining on the nuclear envelope ($p < 0.001$, $n = 25$, Supporting Information Figs. S5C, S6C), visibly reducing the actin connectivity around nucleus. DNKASH and control plasmid groups were subjected to puromycin selection to ensure that cells express the desired constructs (Supporting Information Fig.S7B) **(F)** MSC lysates were probed for Akt phosphorylation (p-Akt; Ser 473). p-Akt was increased threefold ($p < 0.01$) immediately after LMS and after 2 hours p-Akt was reduced 42% ($p < 0.05$) and was not different than control. Similar to FAK, a repeated LMS exposure after 2 hours increased p-Akt 3.7-fold ($p < 0.001$), 46% higher than a single LMS exposure ($p < 0.05$). *, $p < 0.05$; ¥, $p < 0.01$; †, $p < 0.001$, against control and each other. Abbreviations: Ctrl, control; DAPI, 4′,6-diamidino-2-phenylindole; DNKASH, pCDH-EF1-MCS1-puro-mCherry-Nesprin-1αKASH; LMS, low-magnitude mechanical signal; p-FAK, focal adhesion kinase phosphorylation; siSUN, siRNA against SUN-1 and SUN-2; T-FAK, total focal adhesion kinase protein.

inhibitor cytochalasin D (CyD, 0.2 μM) had diminished basal and LMS-induced *p*-FAK (Fig. 2A, $p < 0.001$) but a small LMS response was still measurable ($p < 0.05$). In contrast, inhibiting the RhoA effector protein ROCK (Y27632, 10 μM) to deplete cytoskeletal tension prevented response to LMS (Fig. 2B, $p < 0.001$). The microtubule-specific inhibitor colchicine (Colc, 1 μM), in contrast, did not impair LMS-activation of FAK (Fig. 2C).

Uniaxial strain induces actin stress fibers perpendicular to loading direction [92, 93] while laminar fluid flow induces parallel stress fibers that span the entire cell length [94, 95]. We tested whether LMS induced actin remodeling. 1 hour after LMS, actin remodeling was concentrated at the perinuclear domain, as shown in Figure 2D with increases in both basal and apical surfaces indicating a unique cytoskeletal adaptation arising in the absence of substrate strain [17, 20] (Supporting Information Figs. S2 and S3). Observer blinded counting of cells after LMS treatment showed that twice as many cells displayed visible perinuclear actin fibers (Fig. 2E, $p < 0.01$). We identified the cell for positive perinuclear remodeling whether there was (a) a distinct bright actin ring around the nuclear rim or (b) a distinct and bright accumulation of short actin stress fibers that coincide with the nuclear position.

Decoupling Nucleus from Cytoskeleton by Inhibiting LINC Function Prevents LMS Signaling

The unique LMS-induced perinuclear actin remodeling suggests the presence of LMS generated force at the nucleus. We hypothesized that the LINC scaffold (Fig. 3A) might support the LMS response by providing mechanical coupling between the nucleus and the actin cytoskeleton. Shown in Figure 3B, MSCs treated with a targeted siRNA (siSUN) to deplete SUN nuclear envelope proteins eliminated the LMS-induced FAK response ($p < 0.01$) and decreased basal p-FAK levels (48%, $p < 0.05$). Similarly, overexpression of a dominant negative KASH domain of Nesprin (DNKASH, Supporting Information Fig. S4) that competes for SUN protein binding, ablated the LMS-induced p-FAK response ($p < 0.001$) (Fig. 3C). These results imply that decoupling the nucleus from the actin cytoskeleton interferes with the ability of the cell to respond to vibratory LMS signals.

As expected [63], depleting both SUN1 and SUN2 proteins in MSCs disrupted Nesprin-2 localization to the nuclear envelope (Fig. 3D; Supporting Information Fig. S5B) and decreased Nesprin-2 signal intensity along the major axis of the nuclear envelope (Supporting Information Fig. S5C, 43%, $p < 0.01$). To confirm that our siRNA strategy to disrupt LINC was effective, we showed that siSUN decreased MSC migration (Supporting Information Fig. S7A). Overexpressing DNKASH fragment similarly displaced Nesprin-2 from the nuclear envelope (Fig. 3E; Supporting Information Fig. S6B), leading to reduced Nesprin signal localization (Supporting Information Fig. S6C, 45%, $p < 0.01$). The expression of DNKASH in a homogenous cell population was ensured by puromycin selection of transfected cells before experiments (Supporting Information Fig. S7B).

As activation of Akt is a well-accepted response to mechanical force and is required for the MSC lineage response to HMS [7, 21], we next evaluated the ability of LMS to activate Akt. Similar to FAK activation, LMS activated Akt by three-fold ($p < 0.01$) and a repeated LMS treatment further amplified the Akt phosphorylation (p-Akt) (46%, $p < 0.05$) to 4.4-fold ($p < 0.001$, Fig. 3F). Importantly, preservation of LINC connectivity between the actin cytoskeleton and the nucleus was critical: in cells treated with siSUN or overexpressing DNKASH, LMS failed to activate Akt (Fig. 3G, 3H).

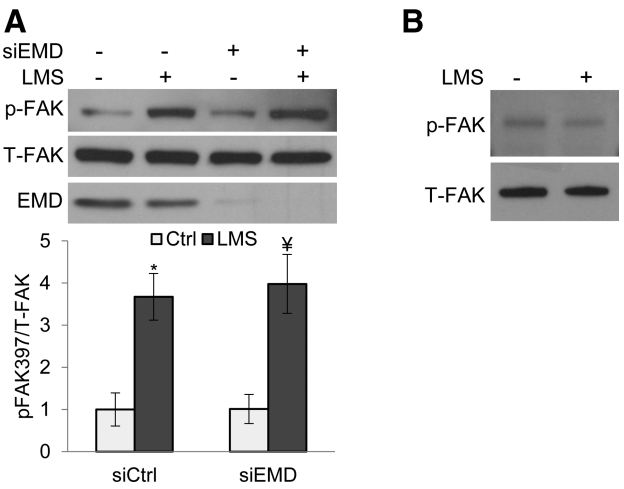

Figure 4. Nuclear envelope protein Emerin does not contribute to low-magnitude mechanical signal (LMS)-induced FAK signaling**. (A):** Marrow-derived MSCs treated with either control siRNA (siCtrl) or Emerin using siRNA (siEMD) were subjected to LMS and probed for focal adhesion kinase phosphorylation (p-FAK) (Tyr 397). Application of LMS increased p-FAK equivalently in both siCtrl (3.6-fold, $p < 0.05$) and siEMD (3.9-fold, $p < 0.01$) groups. Densitometry analysis used data from at least three separate experiments. **(B):** Nuclear envelope proteins were isolated from whole cell lysates immediately after LMS and probed for possible FAK activation. Western blot analysis shows no LMS-induced p-FAK activity at the nuclear envelope. *, $p < 0.05$; ¥, $p < 0.01$; †, $p < 0.001$, against control and each other. Abbreviations: Ctrl, control; EMD, Emerin; LMS, low-magnitude mechanical signal; p-FAK, focal adhesion kinase phosphorylation; siEMD, Emerin using siRNA; T-FAK, total focal adhesion kinase protein.

Recently, nuclear stiffness was shown to be modulated after force applied by Nesprin bound beads, an effect dependent on phosphorylation of the LINC binding partner Emerin (EMD) [78, 96]. To test whether Emerin played a role in LMS induced p-FAK activation, we depleted Emerin using siRNA (siEMD) and found that the signal response to LMS was unaffected (Fig. 4A). Furthermore, probing for p-FAK in isolated nuclear membranes yielded no LMS-induced activity (Fig. 4B), suggesting that FAK activation occurs at a distance from the nucleus. As such, these data suggest that the stiffer and denser cell nucleus might passively participate in the sensation of vibratory signals by virtue of nuclear-cytoskeletal coupling dependent on the LINC complex.

LINC Complex Function Is Required for LMS Repression of Adipogenic Differentiation

To further elucidate the LINC requirement for LMS-induced mechanical signaling, we tested whether LINC function was necessary for the LMS regulation of MSC adipogenesis. When compared with control siRNA (siCtrl), limiting LINC function by siRNA knockdown of both SUN 1 and 2 proteins (siSUN) diminished the transcriptional expression of SUN proteins while increasing the adipocyte specific markers *APN* (287% $p < 0.001$) and *Fatty acid binding protein* 4 (*AP-2*,

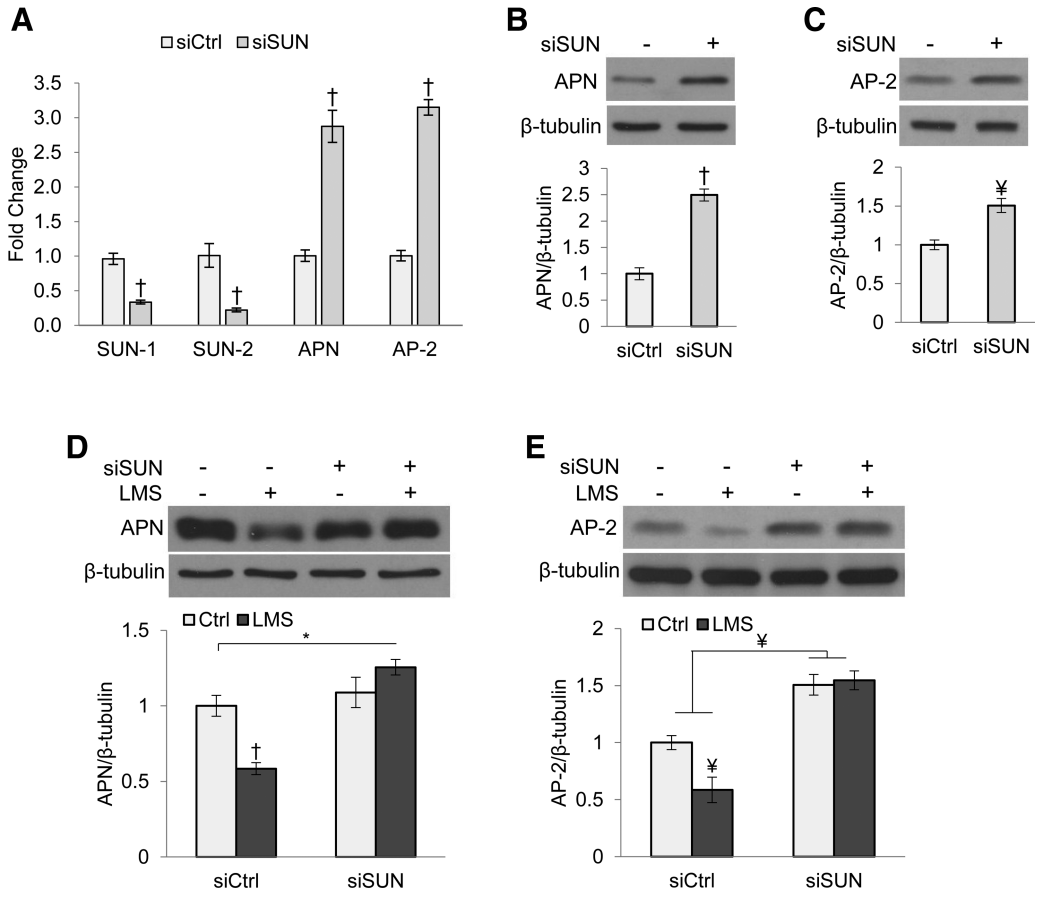

Figure 5. Linker of nucleoskeleton and cytoskeleton complex is required for low-magnitude mechanical signal (LMS) inhibition of adipogenesis. Marrow derived MSCs were plated at a density of 100,000 cells per well into six-well culture plates and treated with siRNA against SUN-1 and SUN-2. Approximately 18 hours after the transfection growth medium was replaced with adipogenic medium containing 0.1 μM dexamethasone and 5 μg/ml insulin. **(A):** After 5 days siRNA against SUN-1 and SUN-2 (siSUN) treated cells showed diminished expression of both *SUN-1* and *2* ($p < 0.001$) and significantly increased expression of known adipogenic markers *adiponectin (APN)* and *AP-2* ($p < 0.001$). Densitometry analysis ($n = 4$) showed increased protein levels of **(B)** APN ($p < 0.001$) and **(C)** AP-2 ($p < 0.01$). Treatment with LMS (0.7 g, 90 Hz, 20 minutes twice daily separated by 2 hours) decreased **(D)** APN ($p < 0.001$) and **(E)** AP-2 ($p < 0.01$) in control siRNA groups consistent with repressed adipogenesis. In siSUN treated cells, decoupling of cytoskeleton from nucleus limited LMS ability to reduce adipogenesis. *, $p < 0.05$; ¥, $p < 0.01$; †, $p < 0.001$, against control and each other. Abbreviations: APN, adiponectin; Ctrl, control; LMS, low-magnitude mechanical signal; siCtrl, control siRNA; siSUN, siRNA against SUN-1 and SUN-2.

315%, $p < 0.001$) after 5 days culture with adipogenic medium, quantified by PCR (Fig. 5A). Immunoblot analysis confirmed increases in adipogenic protein levels of APN (Fig. 5B, 250%, $p < 0.001$) and AP-2 (Fig. 5C, 150%, $p < 0.01$) in SUN knockdown groups. Similarly, cells treated with the dominant negative form of Nesprin KASH domain (DNKASH) demonstrated increases in both gene expression and protein levels of adipogenic markers (Supporting Information Fig. S8A. S8B).

Treatment with LMS (0.7 g, 90 Hz, 20 minutes twice daily separated by 2 hours) for 5 days was sufficient to repress adipogenic markers APN (Fig. 5D, 42%, $p < 0.001$) and AP-2 (Fig. 5E, 43%, $p < 0.01$) in MSCs treated with control siRNA. Importantly, consistent with our finding that LINC functionality is required for LMS-induced mechanoregulation of MSCs, LMS repression of adipogenic differentiation was abrogated when LINC complex was disrupted through siSUN knockdown. DNKASH groups also displayed a restrained LMS effect to decrease adipogenesis (Supporting Information Fig. S8C). Compared with knockdown experiments (Fig. 5A–5C; Supporting Information Fig. S8A, S8B), during LMS experiments, the adipogenic response due to siSUN and DNKASH treatments was less robust (Fig. 5D, 5E; Supporting Information Fig. S8C); adipogenic differentiation might be compromised by the increased handling required for the LMS application protocol where the cultures are removed from optimal incubator conditions into RT.

HMS Signal Generation Does Not Require Functional LINC

We showed that HMS and LMS synergistically increased FAK signaling (Fig. 1G) suggesting a common amplification mechanism through regulation of cell structure. We then asked whether HMS, which inhibits adipogenesis via signals initiated at focal adhesions [10], also required LINC connections or whether the peripheral FA mechanosome was sufficient. Application of HMS increased p-FAK in cells overexpressing DNKASH (1.8-fold, $p < 0.05$, Fig. 6A) or treated with siSUN (1.7-fold, $p < 0.01$, Fig. 6D) indicating that nuclear-cytoskeletal coupling was not critical. Akt signaling was also

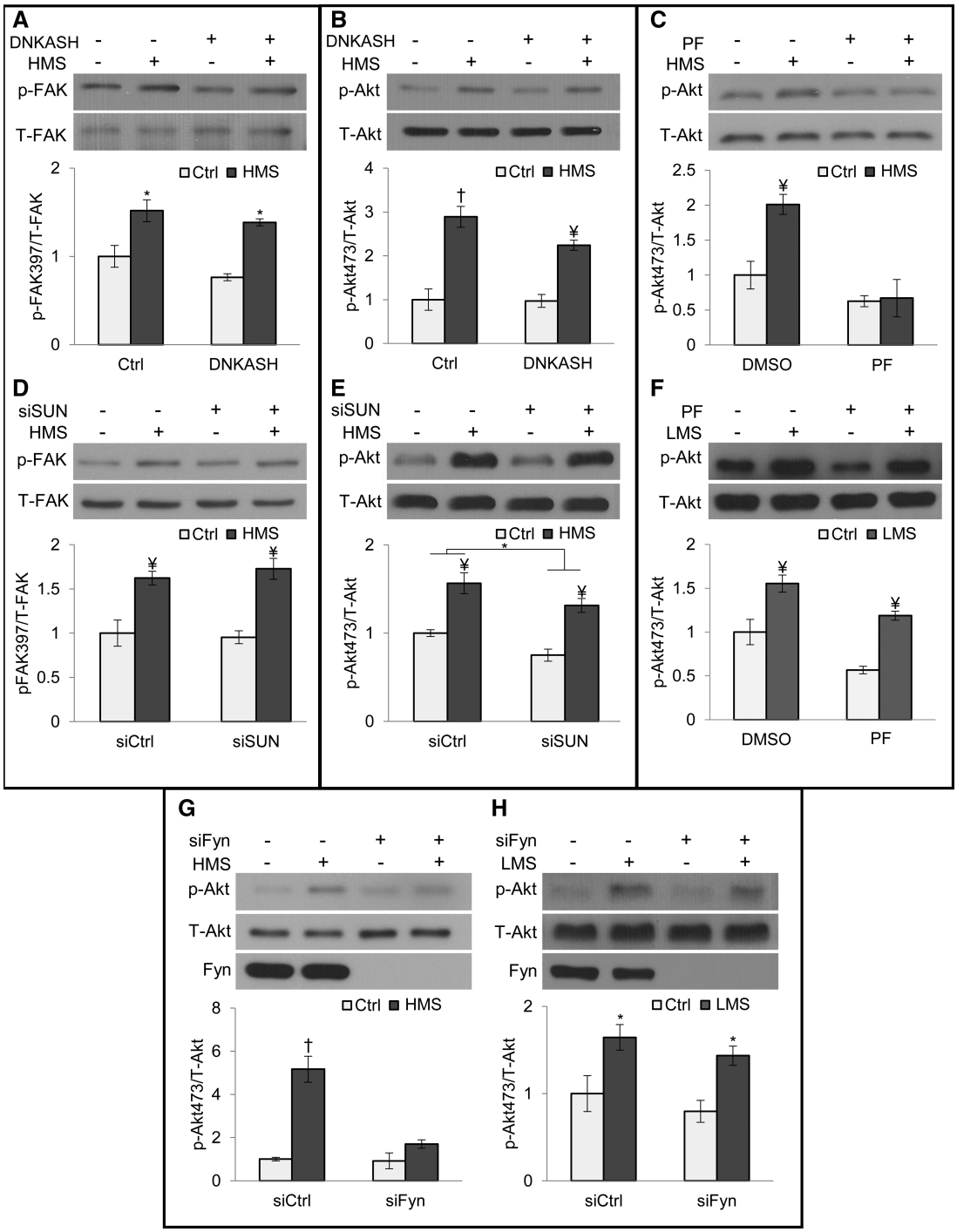

Figure 6. Linker of nucleoskeleton and cytoskeleton is not required for high-magnitude substrate strain (HMS)-induced signaling. HMS activation of focal adhesion kinase phosphorylation (p-FAK) was preserved in both **(A)** pCDH-EF1-MCS1-puro-mCherry-Nesprin-1αKASH (DNKASH) (1.8-fold, $p < 0.05$ and **(D)** siRNA against SUN-1 and SUN-2 (siSUN) (1.7-fold, $p < 0.01$) treated cells. HMS activated Akt phosphorylation (p-Akt) in both **(B)** DNKASH (2.3-fold, $p < 0.01$) and **(E)** siSUN treated cells (1.75-fold, $p < 0.01$). **(C):** FAK inhibitor PF573228 (PF, 3 μM) inhibited strain-induced Akt activation ($p < 0.01$), but **(F)** PF did not inhibit low-magnitude mechanical signal (LMS)-induced p-Akt (two-fold, $p < 0.01$). **(G):** siRNA Fyn knockdown (siFyn) inhibited strain induced p-Akt compared with cells treated with a control siRNA. **(H):** Akt response to LMS was preserved in siFyn cells (1.8-fold, $p < 0.05$). *, $p < 0.05$; ¥, $p < 0.01$; †, $p < 0.001$, against control and each other. Abbreviations: Ctrl, control; DMSO, dimethyl sulphoxide; DNKASH, pCDH-EF1-MCS1-puro-mCherry-Nesprin-1αKASH; HMS, high-magnitude substrate strain; LMS, low-magnitude mechanical signal; p-Akt, Akt phosphorylation; PF, PF573228; p-FAK, focal adhesion kinase phosphorylation; siCtrl, control siRNA; siSUN, siRNA against SUN-1 and SUN-2; T-Akt, total akt protein; T-FAK, total focal adhesion kinase protein.

tested and showed that HMS increased p-Akt despite disruption of nuclear-cytoskeletal tethers by either DNKASH (2.3-fold, $p < 0.01$, Fig. 6B) or siSUN (1.7-fold, $p < 0.01$, Fig. 6E). As such, HMS-induced FAK and Akt signaling did not require mechanical coupling between the nucleus and cytoskeleton.

We considered whether different mechanotransduction mechanisms might be invoked by HMS and LMSs. Interestingly, while proximal FAK activity by HMS was required for subsequent Akt activation (Fig. 6C), it was not required for p-Akt due to LMS (Fig. 6F, $p < 0.01$), emphasizing that different adaptive strategies may result in discrete signaling mechanisms. Further evidence that distinct proximal mechanisms differentiate HMS and LMS was the different requirement for the FAK coregulator, Fyn. Recruitment of Fyn to the FA mechanosome was essential for HMS Akt activation (Fig. 6G) [21], while Fyn depletion did not prevent LMS-induced p-Akt (Fig. 6H, 1.8-fold, $p < 0.05$,).

Discussion

Both LMS and HMSs influence fate selection of MSCs, activating signals that can be tuned to build musculoskeletal tissues and suppress adiposity [1, 4, 5]. Here, we asked whether the LINC complex was involved in transducing relevant regulatory signals. We show that LINC is necessary to allow MSC to respond to low-magnitude high-frequency signals that induce p-FAK and p-Akt and lead to adipogenic repression, but that LINC is not necessary for responses to HMS transmitted at the FA mechanosome. Furthermore, we show that, similar to the ability of the MSC to reorganize its actin cytoskeleton to amplify responses at the FA mechanosome [7, 10], LMS also generates cytoskeletal change. This cytoskeletal reorganization involves not only maturation of the FA mechanosome, which serves to synergistically enhance HMS signaling, but also accrual of a perinuclear actin structure that connects structures of the cytoplasm to the inner nucleus via the LINC complex.

The perinuclear accumulation of F-actin induced by LMS suggests the presence of force at the boundary of the nucleus and the cytoplasmic cytoskeleton. Importantly, mechanically decoupling the nucleus from the cytoskeleton by inhibiting LINC connections disabled the LMS response. Considering the integral function of LINC in providing functional connections between the nucleus and focal adhesions [70], our findings imply that LMS-induced FAK activity is enabled by the LINC-connected nucleus. Although we did not show a direct a physical connection between FAK activity and LINC or measure the level of forces required in this response, limitations of this study, our results strongly demonstrate the importance of the LINC complex in the cellular response to LMS. Furthermore, our previous in silico findings suggest that in response to LMS, the nucleus is capable of generating sufficient mechanical deformation within the cell to serve as a passive, force generating element [26]. Moreover, the lack of FAK activity at the nuclear envelope, and the insensitivity of LMS-induced FAK to knockdown of Emerin (a nuclear envelope protein and LINC partner [96] shown to participate in nuclear stiffness [78]) suggests that FAK signaling is largely due to LMS actions that require connections between the nucleus and the cytoplasmic cytoskeleton. In contrast, HMS-induced FAK and Akt signaling relies exclusively on large substrate deformations and is unaffected by LINC disruption. Finally, our results indicate that in addition to the LINC requirement for LMS-induced signaling, a requirement for proximal Fyn signaling also differed between LMS and HMS, reinforcing that LMS and HMS use divergent signaling modalities.

An alternative physical mechanism by which LMS might initiate signaling is via LMS-induced fluid shear stress. Computational studies revealed that when vibrated at high frequency and low magnitude (30–100 Hz, 0.1–1 g), the relative velocity of solid bodies submerged in the fluid environment can generate fluid shear up to 2 Pa [19, 24] in highly viscous environments like bone marrow (400 cP [97], water is 1 cP). In this study, LMS-induced fluid shear was a function of surface strain (approximately 1.4 $\mu\varepsilon$, Supporting Information Fig. S9A) as the vertical well motion limited the lateral fluid sloshing (Supporting Information Fig. S9B). Our previously validated simulation model [25] predicted a peak velocity differential of approximately 0.00004 m/s (Supporting Information Fig. S9C) corresponding to a LMS-induced fluid shear of 0.0008 Pa (0.008 dyn/cm^2), a level that while comparable with fluid shear required for maintenance of LINC-bound actin cap structures (0.001–0.005 Pa), [72] is two orders magnitudes below that to which bone cells respond [98]. Moreover, this level of shear is insignificant compared with fluid shear generated during handling plates (identical for controls and LMS), particularly when considering the potency of oscillating fluid shear diminished at the higher frequencies [99]. While we cannot exclude the possibility that LMS-induced accelerations works synergistically with fluid shear, we previously did not detect such interactions under much higher shear stresses (5 Pa) where cell responses were associated more strongly with the acceleration magnitude than the LMS-induced fluid shear stress [16, 23, 26]; altogether this suggests that the low level shear generated by LMS is unlikely to be responsible for FAK and Akt activation and subsequent cytoskeletal reorganization as well as repression of adipogenesis.

Differentiation of stem cells requires complex interactions of multiple signaling pathways. We previously showed that adipogenic commitment of MSCs was largely regulated by reduced β-catenin signaling, and that both HMS and LMS impact this pathway during repression of adipogenic commitment [17, 84, 100]. Interestingly, LINC function also affects β-catenin signaling [76]. Here, we demonstrated that limiting LINC functionality by knockdown of SUN1 and SUN2, as well by expressing the dominant negative form of Nesprin KASH domain, increased MSC adipogenesis (Fig. 5A–5C; Supporting Information Fig. S8A, S8B). In agreement with previous work from our laboratory, we found that application of LMS repressed adipogenesis in MSCs in control groups, but when LINC was dysfunctional due to interference with SUN or Nesprin, LMS failed to prevent adipogenesis (Fig. 5; Supporting Information Fig. S8). This indicates that interfering with LMS activation of FAK, Akt, or RhoA, all early events leading to preservation of β-catenin signaling, will also interfere with LMS regulation of MSC differentiation.

In sum, cell signaling in response to extremely small mechanical signals requires LINC complex coupling between the nucleus and cytoskeleton and implicates the LINC interface as a mechanosensory site. We showed for the first time that LMS, an applied physical force that generates neither significant fluid shear (Supporting Information Fig. S9) nor strain [101], activates signaling events inducing FAK, Akt, RhoA, and FA maturation, which have been previously associated with HMS. For the first time we show, at the cellular level, that cytoskeletal adaptations and proximal signaling events initiated by low and high magnitude physical signals differ between LMS and HMS. The LMS-induced cytoskeletal adaptations and requirement for

the LINC interface to support LMS-induced signaling not only provides new insights as to how cells respond to vibratory mechanical information but also shows that perinuclear actin remodeling amplifies the mechanoresponse. Our findings further demonstrated that decreased connectivity between the cell nucleus and cytoplasmic actin impairs anti-adipogenic effects of LMS. With this in mind, it is interesting to consider that, resembling the gradual hearing loss in LINC deficient mice [82], alterations in nuclear-cytoskeletal connections associated with aging or laminopathies like Hutchinson-Gilford progeria [102] might cause a loss in LINC complex-dependent mechanosensitivity to vibratory signals. Such a decrease in mechanosensitivity could potentially contribute to reported failure of musculoskeletal tissues by limiting the accessible spectrum of mechanical information thereby interfering adaptation to functional loading [103]. Translating this to the clinic, physical or chemical interventions that modulate the LINC interface might have the potential to enhance the mechanical sensitivity of an otherwise unresponsive cell population. Finally, our data demonstrate that cells use a multitude of strategies to sense and respond to mechanical signals. While the perception of high-magnitude stimuli appears to rely on signaling at the substrate/membrane interface, extremely low-magnitude mechanical stimuli are detected through the physical connections between nucleus and the cytoskeleton.

Conclusions

Our findings suggest that cellular response to vibration relies on LINC mediated nuclear-cytoplasmic coupling to generate intracellular signaling and influence cell fate. In contrast, signal initiation at focal adhesions due to high magnitude strain is independent of LINC coupling. Vibration induces a unique change in the perinuclear actin cytoskeleton and increases focal adhesions; these cytoskeletal changes amplify mechanical responses due to both high and low magnitude force application. As such, vibration may be useful in treating conditions marked by altered LINC interfaces such as aging, progeriod laminopathies and microgravity.

Acknowledgments

We gratefully appreciate the technical expertise from Lisa Sharek. This study was supported by the National Institutes of Health grants EB014351, AR056655, AR042360, and GM029860.

Author Contributions

G.U.: concept/design, collection/assembly of data, data analysis/interpretation, manuscript writing, final approval of manuscript; W.R.T., B.S., S.S.Y., M.S., C.T.R., S.J., and K.B.: data analysis/interpretation, final approval of manuscript; Z.X., S.M., and G.B.: collection/assembly of data; J.R.: concept/design, financial support, data analysis/interpretation, manuscript writing, final approval of manuscript.

Disclosure of Potential Conflicts of Interest

The authors indicate no potential conflicts of interest.

References

1 Ozcivici E, Luu YK, Adler B et al. Mechanical signals as anabolic agents in bone. Nat Rev Rheumatol 2010;6:50–59.
2 Thompson WR, Rubin CT, Rubin J. Mechanical regulation of signaling pathways in bone. Gene 2012;503:179–193.
3 Sun Y, Chen CS, Fu J. Forcing stem cells to behave: A biophysical perspective of the cellular microenvironment. Ann Rev Biophy 2012;41:519–542.
4 Styner M, Thompson WR, Galior K et al. Bone marrow fat accumulation accelerated by high fat diet is suppressed by exercise. Bone 2014;64:39–46.
5 Shackelford LC, LeBlanc AD, Driscoll TB et al. Resistance exercise as a countermeasure to disuse-induced bone loss. J Appl Physiol 2004;97:119–129.
6 Sordella R, Jiang W, Chen G-C et al. Modulation of Rho GTPase signaling regulates a switch between adipogenesis and myogenesis. Cell 2003;113:147–158.
7 Sen B, Xie Z, Case N et al. mTORC2 Regulates mechanically induced cytoskeletal reorganization and lineage selection in marrow-derived mesenchymal stem cells. J Bone Miner Res 2014;29:78–89.
8 Discher DE, Janmey P, Wang YL. Tissue cells feel and respond to the stiffness of their substrate. Science 2005;310:1139–1143.
9 Hu SH, Chen JX, Butler JP et al. Prestress mediates force propagation into the nucleus. Biochem Biophys Res Commun 2005;329:423–428.
10 Sen B, Guilluy C, Xie Z et al. Mechanically induced focal adhesion assembly amplifies anti-adipogenic pathways in mesenchymal stem cells. Stem Cells 2011;29:1829–1836.
11 Fettiplace R, Hackney CM. The sensory and motor roles of auditory hair cells. Nat Rev Neurosci 2006;7:19–29.
12 Simoni A, Wolfgang W, Topping MP et al. A mechanosensory pathway to the *Drosophila* circadian clock. Science 2014;343:525–528.
13 Rubin C, Turner AS, Bain S et al. Anabolism. Low mechanical signals strengthen long bones. Nature 2001;412:603–604.
14 Gilsanz V, Wren TAL, Sanchez M et al. Low-Level, High-frequency mechanical signals enhance musculoskeletal development of young women with low BMD. J Bone Miner Res 2006;21:1464–1474.
15 Luu YK, Capilla E, Rosen CJ et al. Mechanical stimulation of mesenchymal stem cell proliferation and differentiation promotes osteogenesis while preventing dietary-induced obesity. J Bone Miner Res 2009;24:50–61.
16 Uzer G, Pongkitwitoon S, Ete Chan M et al. Vibration induced osteogenic commitment of mesenchymal stem cells is enhanced by cytoskeletal remodeling but not fluid shear. J Biomech 2013;46:2296–2302.
17 Sen B, Xie Z, Case N et al. Mechanical signal influence on mesenchymal stem cell fate is enhanced by incorporation of refractory periods into the loading regimen. J Biomech 2011;44:593–599.
18 Chan ME, Uzer G, Rubin C. The potential benefits and inherent risks of vibration as a non-drug therapy for the prevention and treatment of osteoporosis. Curr Osteoporos Rep 2013;11:36–44.
19 Dickerson DA, Sander EA, Nauman EA. Modeling the mechanical consequences of vibratory loading in the vertebral body: Microscale effects. Biomech Model Mechanobiol 2008;7:191–202.
20 Garman R, Gaudette G, Donahue LR et al. Low-level accelerations applied in the absence of weight bearing can enhance trabecular bone formation. J Orth Res 2007;25:732–740.
21 Thompson WR, Guilluy C, Xie Z et al. Mechanically activated Fyn utilizes mTORC2 to regulate RhoA and adipogenesis in mesenchymal stem cells. Stem Cells 2013;31:2528–2537.
22 Kearney E, Farrell E, Prendergast P et al. Tensile strain as a regulator of mesenchymal stem cell osteogenesis. Ann Biomed Eng 2010;38:1767–1779.
23 Bacabac RG, Smit TH, Van Loon JJWA et al. Bone cell responses to high-frequency vibration stress: Does the nucleus oscillate within the cytoplasm? FASEB J 2006;20:858–864.
24 Coughlin TR, Niebur GL. Fluid shear stress in trabecular bone marrow due to low-

magnitude high-frequency vibration. J Biomech 2012;45:2222–2229.
25 Uzer G, Manske S, Chan M et al. Separating fluid shear stress from acceleration during vibrations in vitro: Identification of mechanical signals modulating the cellular response. Cell Mol Bioeng 2012;5:266–276.
26 Uzer G, Pongkitwitoon S, Ian C et al. Gap junctional communication in osteocytes is amplified by low intensity vibrations in vitro. PLoS ONE 2014;9:e90840.
27 Rosenberg N, Levy M, Francis M. Experimental model for stimulation of cultured human osteoblast-like cells by high frequency vibration. Cytotechnology 2002;39:125–130.
28 Oxlund BS, Ortoft G, Andreassen TT et al. Low-intensity, high-frequency vibration appears to prevent the decrease in strength of the femur and tibia associated with ovariectomy of adult rats. Bone 2003;32:69–77.
29 Tanaka SM, Li J, Duncan RL et al. Effects of broad frequency vibration on cultured osteoblasts. J Biomech 2003;36:73–80.
30 Verschueren SMP, Roelants M, Delecluse C et al. Effect of 6-month whole body vibration training on hip density, muscle strength, and postural control in postmenopausal women: A randomized controlled pilot study. J Bone Miner Res 2004;19:352–359.
31 Judex S, Zhong N, Squire ME et al. Mechanical modulation of molecular signals which regulate anabolic and catabolic activity in bone tissue. J Cell Biochem 2005;94:982–994.
32 Takeuchi R, Saito T, Ishikawa H et al. Effects of vibration and hyaluronic acid on activation of three-dimensional cultured chondrocytes. Arthritis Rheum 2006;54:1897–1905.
33 Muir J, Judex S, Qin Y et al. Safety of whole body vibration, considered for the prevention and/or treatment of osteoporosis, relative to standards set by the international safety organization. J Bone Miner Res 2006; 21:S294–S294.
34 Xie L, Jacobson JM, Choi ES et al. Low-level mechanical vibrations can influence bone resorption and bone formation in the growing skeleton. Bone 2006;39:1059–1066.
35 Rubin CT, Capilla E, Luu YK et al. Adipogenesis is inhibited by brief, daily exposure to high-frequency, extremely low-magnitude mechanical signals. Proc Natl Acad Sci U S A 2007;104:17879–17884.
36 Prè D, Ceccarelli G, Benedetti L et al. Effects of low-amplitude, high-frequency vibrations on proliferation and differentiation of SAOS-2 human osteogenic cell line. Tissue Eng C Meth 2009;15:669–679.
37 Hwang SJ, Lublinsky S, Seo YK et al. Extremely small-magnitude accelerations enhance bone regeneration: A preliminary study. Clin Orthop Relat Res 2009;467:1083–1091.
38 Sriram D, Jones A, Alatli-Burt I et al. Effects of mechanical stimuli on adaptive remodeling of condylar cartilage. J Dent Res 2009;88:466–470.
39 Holguin N, Muir J, Rubin C et al. Short applications of very low-magnitude vibrations attenuate expansion of the intervertebral disc during extended bed rest. Spine J 2009; 9:470–477.
40 Leung KS, Shi HF, Cheung WH et al. Low-magnitude high-frequency vibration accelerates callus formation, mineralization, and fracture healing in rats. J Orth Res 2009; 27:458–465.
41 Wang CZ, Wang GJ, Ho ML et al. Low-magnitude vertical vibration enhances myotube formation in C2C12 myoblasts. J Appl Physiol 2010;109:840–848.
42 Holguin N, Judex S. Rat intervertebral disc health during hindlimb unloading: Brief ambulation with or without vibration. Aviat Space Environ Med 2010;81:1078–1084.
43 Ozcivici E, Luu YK, Rubin CT et al. Low-level vibrations retain bone marrow's osteogenic potential and augment recovery of trabecular bone during reambulation. PLoS One 2010;5:e11178.
44 Lau E, Lee WD, Li J et al. Effect of low-magnitude, high-frequency vibration on osteogenic differentiation of rat mesenchymal stromal cells. J Orth Res 2011;29:1075–1080.
45 Sandhu E, Miles JD, Dahners LE et al. Whole body vibration increases area and stiffness of the flexor carpi ulnaris tendon in the rat. J Biomech 2011;44:1189–1191.
46 Ito Y, Kimura T, Nam K et al. Effects of vibration on differentiation of cultured PC12 Cells. Biotechnol Bioeng 2011;108:592–599.
47 Pre D, Ceccarelli G, Gastaldi G et al. The differentiation of human adipose-derived stem cells (hASCs) into osteoblasts is promoted by low amplitude, high frequency vibration treatment. Bone 2011;49:295–303.
48 Holguin N, Uzer G, Chiang FP et al. Brief daily exposure to low-intensity vibration mitigates the degradation of the intervertebral disc in a frequency-specific manner. J Appl Physiol 2011;111:1846–1853.
49 Tirkkonen L, Halonen H, Hyttinen J et al. The effects of vibration loading on adipose stem cell number, viability and differentiation towards bone-forming cells. J R Soc Interface 2011;8:1736–1747.
50 Zhou Y, Guan X, Zhu Z et al. Osteogenic differentiation of bone marrow-derived mesenchymal stromal cells on bone-derived scaffolds: Effect of microvibration and role of ERK1/2 activation. Eur Cell Mater 2011;22: 12–25.
51 Isachenko V, Maettner R, Sterzik K et al. In-vitro culture of human embryos with mechanical micro-vibration increases implantation rates. Reprod Biomed Online 2011;22: 536–544.
52 Kim IS, Song YM, Lee B et al. Human mesenchymal stromal cells are mechanosensitive to vibration stimuli. J Dent Res 2012; 91:1135–1140.
53 Fung EB, Gariepy CA, Sawyer AJ et al. The effect of whole body vibration therapy on bone density in patients with thalassemia: A pilot study. Am J Hematol 2012;87:E76–E79.
54 El-Shamy SM. Effect of whole-body vibration on muscle strength and balance in diplegic cerebral palsy: A Randomized controlled trial. Am J Phys Med Rehab 2014;93: 114–121 110.1097/PHM.1090b1013e3182a1541a1094.
55 Demiray L, Özçivici E. Bone marrow stem cells adapt to low-magnitude vibrations by altering their cytoskeleton during quiescence and osteogenesis. Turkish J Biol 2015; 39:88–97.
56 Burridge K, Wittchen ES. The tension mounts: Stress fibers as force-generating mechanotransducers. J Cell Biol 2013;200:9–19.
57 McBeath R, Pirone DM, Nelson CM et al. Cell Shape, Cytoskeletal tension, and RhoA regulate stem cell lineage commitment. Dev Cell 2004;6:483–495.
58 Wang N, Butler JP, Ingber DE. Mechanotransduction across the cell-surface and through the cytoskeleton. Science 1993;260: 1124–1127.
59 Francois M, Baldi J, Manning P et al. 'Exercise snacks' before meals: A novel strategy to improve glycaemic control in individuals with insulin resistance. Diabetologia 2014: 1–9.
60 Martins RP, Finan JD, Farshid G et al. Mechanical regulation of nuclear structure and function. Annu Rev Biomed Eng 2012;14: 431–455.
61 Engler AJ, Sen S, Sweeney HL et al. Matrix elasticity directs stem cell lineage specification. Cell 2006;126:677–689.
62 Dupont S, Morsut L, Aragona M et al. Role of YAP/TAZ in mechanotransduction. Nature 2011;474:179–183.
63 Crisp M, Liu Q, Roux K et al. Coupling of the nucleus and cytoplasm: Role of the LINC complex. J Cell Biol 2006;172:41–53.
64 Lombardi ML, Jaalouk DE, Shanahan CM et al. The interaction between nesprins and sun proteins at the nuclear envelope is critical for force transmission between the nucleus and cytoskeleton. J Biol Chem 2011; 286:26743–26753.
65 Zhang Q, Skepper JN, Yang F et al. Nesprins: A novel family of spectrin-repeat-containing proteins that localize to the nuclear membrane in multiple tissues. J Cell Sci 2001;114:4485–4498.
66 Zhen Y-Y, Libotte T, Munck M et al. NUANCE, a giant protein connecting the nucleus and actin cytoskeleton. J Cell Sci 2002;115:3207–3222.
67 Stewart-Hutchinson PJ, Hale CM, Wirtz D et al. Structural requirements for the assembly of LINC complexes and their function in cellular mechanical stiffness. Exp Cell Res 2008;314:1892–1905.
68 Lu W, Schneider M, Neumann S et al. Nesprin interchain associations control nuclear size. Cell Mol Life Sci 2012;69:3493–3509.
69 Kanchanawong P, Shtengel G, Pasapera AM et al. Nanoscale architecture of integrin-based cell adhesions. Nature 2010;468:580–584.
70 Fedorchak GR, Kaminski A, Lammerding J. Cellular mechanosensing: Getting to the nucleus of it all. Prog Biophys Mol Biol. 2014;115:76–92.
71 Nagayama K, Yahiro Y, Matsumoto T. Apical and basal stress fibers have different roles in mechanical regulation of the nucleus in smooth muscle cells cultured on a substrate. Cell Mol Bioeng 2013;6:473–481.
72 Chambliss AB, Khatau SB, Erdenberger N et al. The LINC-anchored actin cap connects the extracellular milieu to the nucleus for ultrafast mechanotransduction. Sci Rep 2013; 3:1087.
73 Poh Y-C, Shevtsov SP, Chowdhury F et al. Dynamic force-induced direct dissocia-

tion of protein complexes in a nuclear body in living cells. Nat Commun 2012;3:866.
74 Swift J, Ivanovska IL, Buxboim A et al. Nuclear Lamin-A scales with tissue stiffness and enhances matrix-directed differentiation. Science 2013;341:1240104.
75 Zwerger M, Jaalouk DE, Lombardi ML et al. Myopathic lamin mutations impair nuclear stability in cells and tissue and disrupt nucleo-cytoskeletal coupling. Hum Mol Genet 2013;22:2335–2349.
76 Neumann S, Schneider M, Daugherty RL et al. Nesprin-2 interacts with α-Catenin and regulates Wnt signaling at the nuclear envelope. J Biol Chem 2010;285:34932–34938.
77 Rashmi RN, Eckes B, Glöckner G et al. The nuclear envelope protein Nesprin-2 has roles in cell proliferation and differentiation during wound healing. Nucleus 2012;3:172–186.
78 Guilluy C, Osborne LD, Van Landeghem L et al. Isolated nuclei adapt to force and reveal a mechanotransduction pathway in the nucleus. Nat Cell Biol 2014;16:376–381.
79 Wang N, Tytell JD, Ingber DE. Mechanotransduction at a distance: Mechanically coupling the extracellular matrix with the nucleus. Nat Rev Mol Cell Biol 2009;10:75–82.
80 Nagayama K, Yamazaki S, Yahiro Y et al. Estimation of the mechanical connection between apical stress fibers and the nucleus in vascular smooth muscle cells cultured on a substrate. J Biomech 2014;11:1422–1429.
81 Wang X, Ha T. Defining single molecular forces required to activate integrin and notch signaling. Science 2013;340:991–994.
82 Horn HF, Brownstein Z, Lenz DR et al. The LINC complex is essential for hearing. J Clin Invest 2013;123:740–750.
83 Peister A, Mellad JA, Larson BL et al. Adult stem cells from bone marrow (MSCs) isolated from different strains of inbred mice vary in surface epitopes, rates of proliferation, and differentiation potential; 2004;103: 1662–1668.
84 Case N, Xie Z, Sen B et al. Mechanical activation of β-catenin regulates phenotype in adult murine marrow-derived mesenchymal stem cells. J Orth Res 2010;28:1531–1538.
85 Lammerding J, Schulze PC, Takahashi T et al. Lamin A/C deficiency causes defective nuclear mechanics and mechanotransduction. J Clin Invest 2004;113:370–378.
86 Kuo J-C, Han X, Yates J, III et al. Isolation of focal adhesion proteins for biochemical and proteomic analysis. In: Shimaoka M, ed. Integrin and Cell Adhesion Molecules. Humana Press; Methods Mol Biol 2012;757:297–323.
87 Liu BP, Burridge K. Vav2 Activates Rac1, Cdc42, and RhoA downstream from growth factor receptors but Not β1 integrins. Mol Cell Biol 2000;20:7160–7169.
88 Arthur WT, Burridge K. RhoA Inactivation by p190RhoGAP regulates cell spreading and migration by promoting membrane protrusion and polarity. Mol Biol Cell 2001;12: 2711–2720.
89 Razafsky DS, Ward CL, Kolb T et al. Developmental regulation of linkers of the nucleoskeleton to the cytoskeleton during mouse postnatal retinogenesis. Nucleus 2013;4:399–409.
90 Mitra SK, Hanson DA, Schlaepfer DD. Focal adhesion kinase: In command and control of cell motility. Nat Rev Mol Cell Biol 2005;6:56–68.
91 Schober M, Raghavan S, Nikolova M et al. Focal adhesion kinase modulates tension signaling to control actin and focal adhesion dynamics. J Cell Biol 2007;176:667–680.
92 Pan J, Wang T, Wang L et al. Cyclic strain-induced cytoskeletal rearrangement of human periodontal ligament cells via the Rho signaling pathway. PLoS ONE 2014;9:e91580.
93 Greiner AM, Chen H, Spatz JP et al. Cyclic Tensile strain controls cell shape and directs actin stress fiber formation and focal adhesion alignment in spreading cells. PLoS ONE 2013;8:e77328.
94 Mott RE, Helmke BP. Mapping the dynamics of shear stress-induced structural changes in endothelial cells. 2007;293: C1616–C1626.
95 Noria S, Xu F, McCue S et al. Assembly and reorientation of stress fibers drives morphological changes to endothelial cells exposed to shear stress. Am J Pathol 2004; 164:1211–1223.
96 Berk JM, Tifft KE, Wilson KL. The nuclear envelope LEM-domain protein emerin. Nucleus 2013;4:298–314.
97 Gurkan UA, Akkus O. The mechanical environment of bone marrow: A review. Ann Biomed Eng 2008;36:1978–1991.
98 Klein-Nulend J, van der Plas A, Semeins CM et al. Sensitivity of osteocytes to biomechanical stress in vitro. FASEB J 1995;9:441–445.
99 Donahue SW, Jacobs CR, Donahue HJ. Flow-induced calcium oscillations in rat osteoblasts are age, loading frequency, and shear stress dependent. Am J Physiol Cell Physiol 2001;281:C1635–C1641.
100 Sen B, Styner M, Xie Z et al. Mechanical loading regulates NFATc1 and β-Catenin signaling through a GSK3β control node. J Biol Chem 2009;284:34607–34617.
101 Judex S, Lei X, Han D et al. Low-magnitude mechanical signals that stimulate bone formation in the ovariectomized rat are dependent on the applied frequency but not on the strain magnitude. J Biomech 2007;40: 1333–1339.
102 Scaffidi P, Misteli T. Lamin A-dependent nuclear defects in human aging. Science 2006;312:1059–1063.
103 Rubin C, Recker R, Cullen D et al. Prevention of postmenopausal bone loss by a low-magnitude, high-frequency mechanical stimuli: A clinical trial assessing compliance, efficacy, and safety. J Bone Miner Res 2004;19:343–351.


See www.StemCells.com for supporting information available online.